



Efficient priors for Multi-frame and Single-frame Super Resolution

Pulak Purkait

SRF, ECSU, Indian Statistical Institute
Kolkata

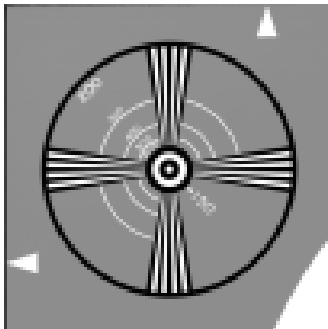
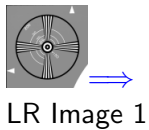
pulak_r@isical.ac.in

August 11, 2012

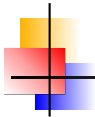




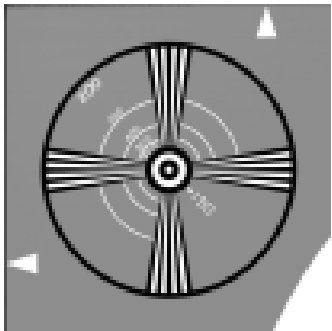
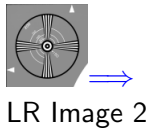
What is Super Resolution?



Bicubic Interpolated Image



What is Super Resolution?



Bicubic Interpolated Image

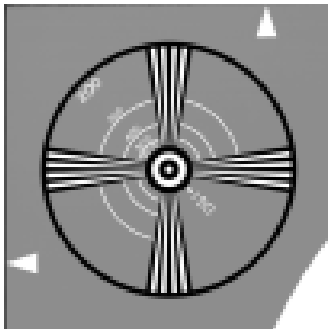




What is Super Resolution?

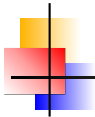


LR Image 3

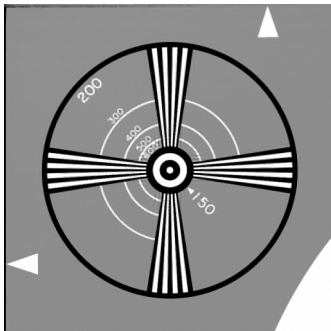
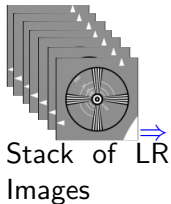


Bicubic Interpolated Image





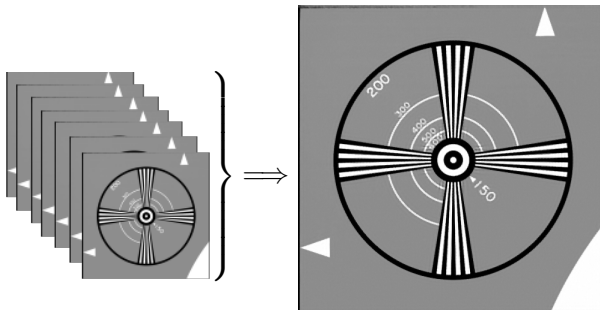
What is Super Resolution?



Super Resolution Image.

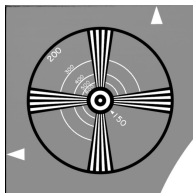
What is Super Resolution?

Definition: Super-resolution is largely known as a technique whereby multi-frame motion is used to overcome the inherent resolution limitations of a low resolution camera system.



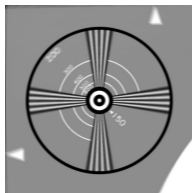
Estimated High Resolution Image [11].

Block diagram representation



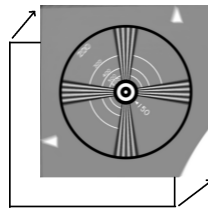
Real World Scene

H_{atm}



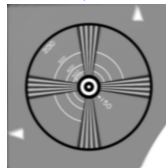
Atmospheric Blur Effect

F_k



Motion Effect

$H_{cam} \downarrow$



D

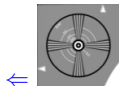
Camera Blur Effect



Noisy, Blurred,
Down-sampled
Out-come

e_k

Out-



Down-sampling
Effect



Model Construction

$$\mathbf{Y}_k = DF_k H \mathbf{X} + \mathbf{e}_k, \quad \forall k = 1, 2, \dots, K$$

| Known: | Symbols: | Represents: |
|--------|----------------|---------------------------------|
| ✓ | \mathbf{Y}_k | k^{th} LR Image |
| ✗ | \mathbf{X} | HR Image |
| ✓ | D | Decimation Matrix |
| ✗ | F_k | Geometric Transformation Matrix |
| ✗ | H | Blurring Kernel |
| ✗ | \mathbf{e}_k | Random Noise |
| ✓ | K | Number of LR images |

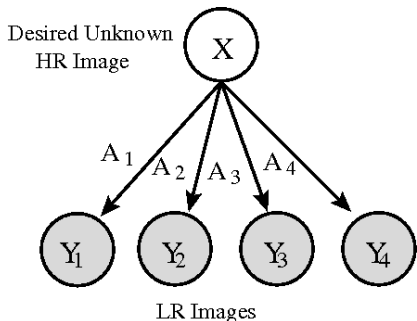


$$\mathbf{Y}_k = D\mathbf{F}_k\mathbf{H}\mathbf{X} + \mathbf{e}_k, \quad \forall k = 1, 2, \dots, K$$

| Known: | Symbols: | Represents: |
|--------|----------------|----------------------------------------------|
| ✓ | \mathbf{Y}_k | k^{th} LR Image |
| ✗ | \mathbf{X} | HR Image \leftarrow Predict |
| ✓ | D | Decimation Matrix |
| ✓ | \mathbf{F}_k | Geometric Transformation Matrix ^a |
| ✓ | H | Blurring Kernel |
| ✗ | \mathbf{e}_k | Random Noise |
| ✓ | K | Number of LR images |

^aVandewalle et al., A frequency domain approach to registration of aliased images with application to super-resolution, EURASIP, 2006.

Generative Model Representation



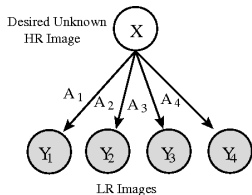
In our case it is not a fully generative model as we assumed some model parameters. Shaded circles are observed variables. $A_k = DF_k H$ are the weights corresponding to LR image Y_k .

Maximum a Posteriori (MAP) solution

$$F = \underbrace{\frac{1}{2\sigma^2} \sum_{k=1}^K \rho(Y_k, A_k X)}_{\text{Likelihood}} - \underbrace{\log(p(X))}_{\text{prior}}$$

Standard method: Assume $\rho(Y_k, A_k X) = \|Y_k - A_k X\|_2^2$, $p(X) = \exp\{-\Upsilon(X)\}$, and $\Upsilon(X) = |\Gamma(X)|$ solve the above using gradient descent.

$$\frac{\partial F}{\partial X} = -\frac{1}{2\sigma^2} \sum_{k=1}^K A_k^T (Y_k - A_k X) - \frac{\partial}{\partial X} \Gamma(X)$$



SR reconstruction Model:

$$Y_k = A_k X + e_k, \quad \forall k = 1, 2, \dots, K$$

LSE technique would give the solution of the form :

$$\hat{X} = \arg \min_X \left[\sum_{k=1}^K \|Y_k - A_k X\|_2^2 \right]$$

For unique solution, we add a regularization term $\Upsilon(X)$ as:

$$\hat{X} = \arg \min_X \left[\sum_{k=1}^K \|Y_k - A_k X\|_2^2 + \lambda \Upsilon(X) \right]$$

where λ is a regularization parameter and $\Upsilon(X) = |\Gamma(X)|_1$. This method is popularly known as LSE with TV regularization.



SR reconstruction Model:

$$\hat{X} = \arg \min_X \left[\sum_{k=1}^K \|Y_k - A_k X\|_2^2 + \lambda \Upsilon(X) \right]$$

We investigate on following:

- ▶ We develop a locally adaptive regularization parameter λ from multi-scale morphological Gain-map [7] .
- ▶ We use non-linear multi-scale morphological gradient operator $\Upsilon(X)$ and then solve the convex problem by formulating efficient subgradients of morphological operators [11].
- ▶ We show the relationship between a non-linear edge-preserving filtering and a regularization technique that leads to a geodesic kernel smoother for super resolution [10].

Single-frame Super Resolution: only one LR image is available.
(Sometimes it is called as model based zooming)

We also investigate on following:

- ▶ Learn image prior from a database of natural images. Learn the correspondence of patch pairs of LR and HR images by multiple sparse dual Dictionary Learning [9].
- ▶ Learn the patch prior from the image itself using local self-similarity in multiple scales without help of any external database of natural images [8].



Chapter I: SR reconstruction using locally adaptive regularization with morphologic gain map



General SR reconstruction Model:

$$\hat{X} = \arg \min_X \left[\sum_{k=1}^K \|Y_k - A_k X\|_p^p + \lambda \Upsilon(X) \right]$$

where $1 \leq p \leq 2$, $\Upsilon(X) = \|\Gamma(X)\|$ and Γ is a high frequency operator.

Different types of regularization:

- ▶ $\Upsilon(X) = |\nabla X|_2^2$ known as bounded variation (BV) regularization.
- ▶ $\Upsilon(X) = |\nabla X|_1$ known as total variation (TV) regularization.
- ▶ $\Upsilon(X) = \sum_{l=-w}^w \sum_{m=-w}^w \alpha^{|l|+|m|} |X - S_x^l S_y^m X|$ known as bilateral total variation (BTV) regularization, where $l + m \geq 0$ and S_x^l, S_y^m are shift-operators along x and y directions with l and m pixel respectively.

▶ BV / TV : $\Gamma = \nabla_x + \nabla_y$

$$= \begin{bmatrix} -1 & 1 \end{bmatrix} + \begin{bmatrix} -1 \\ 1 \end{bmatrix}$$

▶ BTV : $\Gamma = \alpha \left(\begin{bmatrix} -1 & 1 \end{bmatrix} + \begin{bmatrix} -1 \\ 1 \end{bmatrix} \right)$

$$+ \alpha^2 \left(\begin{bmatrix} -1 & 0 & 1 \end{bmatrix} + \begin{bmatrix} -1 \\ 0 \\ 1 \end{bmatrix} \right)$$

...



The modified ART like algorithm [1] using BTV regularization ¹:

$$X_j^{(n+1)} = X_j^{(n)} + \beta^{(n)} \frac{(A_{k,j})^T}{\|A_{k,j}\|^2} \text{sign}(\mathbf{Y}_k - A_k \mathbf{X}^{(n)}) +$$

$$\lambda \underbrace{\sum_{l=-w}^w \sum_{m=-w}^w}_{l+m \geq 0} \alpha^{|m|+|l|} [I - S_y^{-m} S_x^{-l}] \text{sign}(X^n - S_x^l S_y^m X^n)$$

for $j = 0, 1, 2, \dots, N-1$ and $k = 0, 1, 2, \dots, K-1$

Here both the terms data term and regularization terms taken as l_1 norm.

¹S. Farsiu, M. D. Robinson, M. Elad, and P. Milanfar. Fast and robust multi-frame super-resolution. IEEE Transactions on Image Processing, 13(10):13271344, October 2004.

Reconstruction Result



Output with BTV regularization, with 10 LR images upsampled
 5×5 times [noise variation $\sigma = 5$].



Our observation

- ▶ Noise and Edges both contribute high-frequency components.
 - # Both suppressed or enhanced during reconstruction process.
- ▶ A periodic ringing noise appears parallel to the edges in the estimated image.
 - # Most distracting in smooth regions.

Possible Solution:

Employ some adaptive technique where the relative effect at each iteration is controlled by a gain map at each pixel depending upon its neighbourhood information.



Proposed Solution

$$\begin{aligned}
 \mathbf{X}_j^{(n+1)} = & \mathbf{X}_j^{(n)} + \beta^{(n)} \left[\underbrace{[\omega I(j,j) + (1-\omega)I_{gain}^{(p)}(j,j)]}_{\text{Weight for Data term}} \right. \\
 & \times \frac{(A_{k,j})^T}{\|A_{k,j}\|^2} \text{sign}(\mathbf{Y}_k - A_k \mathbf{X}) + \underbrace{[I(j,j) - I_{gain}^{(p)}]}_{\text{Weight for Regularization term}} \\
 & \times \underbrace{\sum_{l=-w}^w \sum_{m=-w}^w}_{l+m \geq 0} \alpha^{|m|+|l|} [I - S_y^{-m} S_x^{-l}] \text{sign}(\mathbf{X}^{(n)} - S_x^l S_y^m \mathbf{X}^{(n)}) \left. \right], \\
 & \text{for } j = 0, 1, 2, \dots, N-1 \text{ and } k = 0, 1, 2, \dots, K-1
 \end{aligned}$$



Idea behind the gain map I_{gain} formulation:

- ▶ It should be small in smooth region (ideally zero) and large along the edge or boundary (ideally one).
- ▶ Robust to noise: should be small in the noisy pixels in smooth region even if it contains high-frequency.

We use morphological operators to compute gain map I_{gain} .

Morphological opening and closing remove bright and dark noise pixel respectively, without effecting edges.

Algorithm to compute I_{gain} :

Step 1: Initialize image $F = \mathbf{0}$.

Step 2: Iterate the following steps for $r = 1$ to m

▶ $F_1 = X^n \circ rS$

$F_2 = X^n \bullet rS$

▶ $F_1 = F_1 \ominus rS$

▶ $F_2 = F_2 \oplus rS$

▶ Calculate intermediate gradient image

$F = F + (F_2 - F_1)$

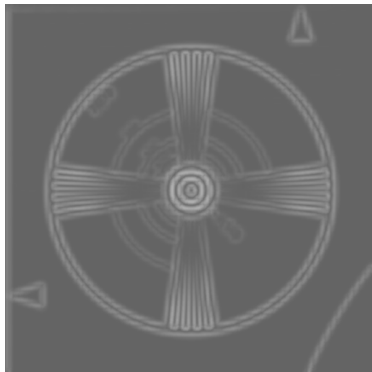
Step 3: $F(i,j) = \text{Sigmoid} \left(F(i,j) - \frac{F_{max} + F_{min}}{2} \right)$, where

$$\text{Sigmoid}(x) = \frac{1}{1 + e^{-\sigma x}}$$

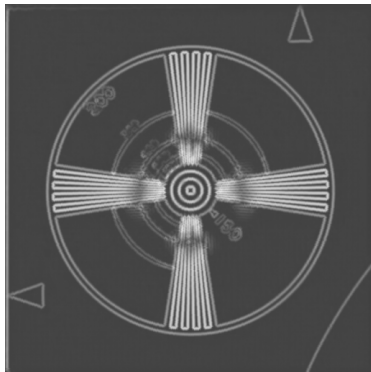
Step 4: $dia(I_g) = F$.



Example of gain map

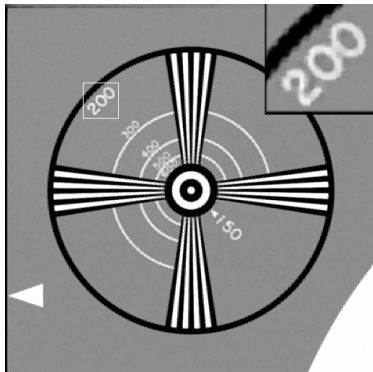


gain map after 1st iteration

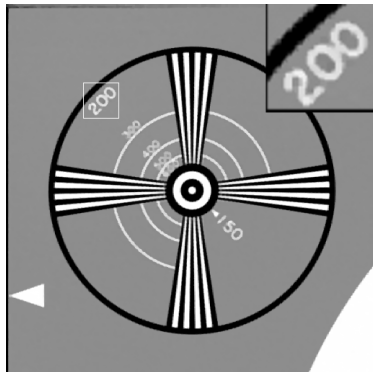


gain map after 10th iteration

SR image reconstruction



BTV regularization(PSNR=29.56)



Proposed regularization(PSNR=30.69)



SR image reconstruction

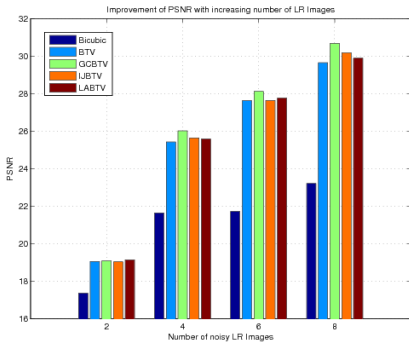


BTV regularization(PSNR=29.65)

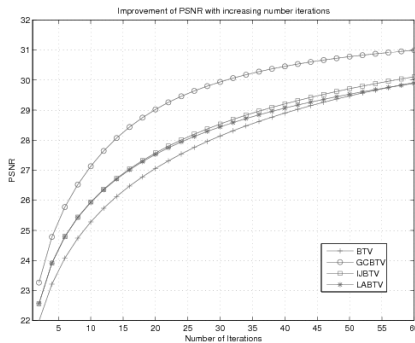


Proposed regularization(PSNR=30.01)

PSNR Plot diagrams



PSNR Vs. # LR images



PSNR Vs. # Iteration



Chapter II: Fast SR reconstruction with Morphological Regularization





Revisit different Regularization Methods:

General SR reconstruction Model:

$$\hat{X} = \arg \min_X \left[\sum_{k=1}^K \|Y_k - A_k X\|_p^p + \lambda \Upsilon(X) \right]$$

where $1 \leq p \leq 2$, $\Upsilon(X) = \|\Gamma(X)\|$ and Γ is a high frequency operator.

Different types of regularization:

- ▶ $\Upsilon(X) = |\nabla X|_2^2$ known as bounded variation (BV) regularization.
- ▶ $\Upsilon(X) = |\nabla X|_1$ known as total variation (TV) regularization.
- ▶ $\Upsilon(X) = \sum_{l=-w}^w \sum_{m=-w}^w \alpha^{|l|+|m|} |X - S_x^l S_y^m X|$ known as bilateral total variation (BTV) regularization. Where $l + m \geq 0$ and S_x^l, S_y^m are shift-operators along x and y directions with l and m pixel respectively.

Motivation:

- ▶ Existing regularization techniques are only based on direct image gradients.
- ▶ Exploring different feature based regularization technique.
- ▶ The last work suggesting that morphological operators could be a great choice.

Difficulty:

- ▶ Highly non-linearity makes the problem difficult to handle.
- ▶ Needs to calculate the subgradients for morphological operators.
- ▶ Slower than calculating direct derivatives.



Difficulty: Possible Solution

- ▶ Highly non-linearity makes the problem difficult to handle.
 - # Non-linear is good because it can be made locally adaptive
- ▶ Needs to calculate the subgradients for morphological operators.
 - # We calculate Morphological subgradients efficiently
- ▶ Slower than calculating direct derivatives.
 - # We develop advanced Bregman iteration for super resolution problem instead of gradient descent.

Proposed Morphological Regularization

$$\Upsilon(\mathbf{X}) = \sum_{s=1}^S \alpha^s \mathbf{1}^t [C_s(\mathbf{X}) - O_s(\mathbf{X})]$$

where $O_s(\mathbf{X}) = D_s(E_s(\mathbf{X}))$, $C_s(\mathbf{X}) = E_s(D_s(\mathbf{X}))$

$$D_s(\mathbf{X}) = \begin{pmatrix} \max_{r \in (sB)_{(1)}} \{X_r\} \\ \max_{r \in (sB)_{(2)}} \{X_r\} \\ \vdots \\ \max_{r \in (sB)_{(mn)}} \{X_r\} \end{pmatrix}, \quad E_s(\mathbf{X}) = \begin{pmatrix} \min_{r \in (sB)_{(1)}} \{X_r\} \\ \min_{r \in (sB)_{(2)}} \{X_r\} \\ \vdots \\ \min_{r \in (sB)_{(mn)}} \{X_r\} \end{pmatrix}$$

Bregman Iteration:

Consider the following minimization problem:

$$\min_{\mathbf{X}} \{\Upsilon(\mathbf{X}) : T(\mathbf{X}) = 0\}$$

Now the Bregman iterations that solve the above constrained minimization problem are as follows:

Initialize $\mathbf{X}^0 = \mathbf{p}^0 = \mathbf{0}$

$$\begin{cases} \mathbf{X}^{(n+1)} = \arg \min_{\mathbf{X}} \{\mu B_{\Upsilon}^{\mathbf{p}^{(n)}}(\mathbf{X}, \mathbf{X}^{(n)}) + T(\mathbf{X})\} \\ \mathbf{p}^{(n+1)} = \mathbf{p}^{(n)} - \nabla T(\mathbf{X}^{(n+1)}) \end{cases}$$

where $B_{\Upsilon}^{\mathbf{p}^{(n)}}$ is the Bregman distance corresponding to convex functional $\Upsilon(\cdot)$ and is defined from point \mathbf{X} to point \mathbf{V} as

$$B_{\Upsilon}^{\mathbf{p}}(\mathbf{X}, \mathbf{V}) = \Upsilon(\mathbf{X}) - \Upsilon(\mathbf{V}) - \langle \mathbf{p}, \mathbf{X} - \mathbf{V} \rangle$$

Proximal Map:

Consider the following unconstrained minimization problem:

$$\min_{\mathbf{X}} (\mu \Upsilon(\mathbf{X}) + T(\mathbf{X}))$$

The solution satisfies the condition:

$$\mu \partial \Upsilon(\mathbf{X}) + \partial T(\mathbf{X}) = 0 \Rightarrow (\mathbf{X} + \gamma \mu \partial \Upsilon(\mathbf{X})) - (\mathbf{X} - \gamma \partial T(\mathbf{X})) = 0$$

This leads to a forward and backward splitting algorithm:

$$\mathbf{X}^{(k+1)} = \text{Prox}_{\Upsilon}(\mathbf{X}^{(k)} - \gamma \partial T(\mathbf{X}^{(k)})),$$

where the proximal operator $\text{Prox}_{\Upsilon}(\mathbf{V})$ is defined as:

$$\text{Prox}_{\Upsilon}(\mathbf{V}) = \arg \min_{\mathbf{X}} \{ \mu \Upsilon(\mathbf{X}) + \frac{1}{2\gamma} \|\mathbf{X} - \mathbf{V}\|_2^2 \}$$

Super resolution unconstrained minimization Problem:

$$\hat{\mathbf{X}} = \arg \min_{\mathbf{X}} \{ \Upsilon(\mathbf{X}) : \|R\mathbf{H}\mathbf{X} - \underline{\mathbf{Y}}\|_2^2 < \eta \}$$

The proposed SR image reconstruction algorithm combining Bregman iteration and operator splitting as follows:

Proposed Iterative Algorithm:

Initialize $\mathbf{Y}^{(0)} = \underline{\mathbf{Y}}, \mathbf{X}^{(0)} = \text{FillUnknown}(\underline{\mathbf{Y}})$;

$$\begin{aligned} & \text{While}(\|R\mathbf{H}\mathbf{X}^{(n)} - \underline{\mathbf{Y}}\|_2^2 > \eta) \\ & \quad \begin{cases} \mathbf{U}^{(n+1)} = \mathbf{X}^{(n)} - \gamma \mathbf{H}^T \mathbf{R}^T (R\mathbf{H}\mathbf{X}^{(n)} - \underline{\mathbf{Y}}) \\ \mathbf{X}^{(n+1)} = \mathbf{U}^{(n+1)} - \mu' \left| \frac{\delta \Upsilon(\mathbf{X})}{\delta \mathbf{X}} \right|_{\mathbf{X}^{(n)}} \\ \mathbf{Y}^{(n+1)} = \underline{\mathbf{Y}} + (\underline{\mathbf{Y}} - R\mathbf{H}\mathbf{X}^{(n+1)}) \end{cases} \\ & \quad n = n + 1 \\ & \text{end} \end{aligned} \tag{1}$$

Efficient computation of $\left| \frac{\delta \Upsilon(\mathbf{X})}{\delta \mathbf{X}} \right|$: Using Chain Rule

$$\Upsilon(\mathbf{X}) = \sum_{s=1}^S \alpha^s \mathbf{1}^t [C_s(\mathbf{X}) - O_s(\mathbf{X})],$$

where $O_s(\mathbf{X}) = D_s(E_s(\mathbf{X}))$, $C_s(\mathbf{X}) = E_s(D_s(\mathbf{X}))$

$$D_s(X) = (X \oplus B) \oplus \dots \oplus B = D(D(\dots s \text{ times } \dots D(X) \dots))$$

$$\begin{aligned} \frac{\delta}{\delta X} D_s(X) &= \frac{\delta}{\delta X} [D(D_{s-1}(X))] \\ &= \frac{\delta D_s}{\delta D_{s-1}} \frac{\delta D_{s-1}}{\delta D_{s-2}} \dots \frac{\delta D_1(X)}{\delta X} \end{aligned}$$

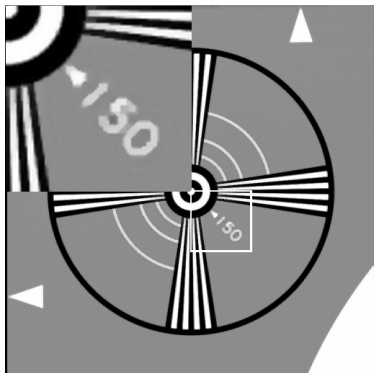
Let $Z^{d_1} = \frac{\delta D}{\delta X} \mathbf{1}$ and $Z^{e_1} = \frac{\delta E}{\delta X} \mathbf{1}$

$$\begin{aligned} Z^{d_s} &:= \frac{\delta}{\delta X} [D_s(X)] \mathbf{1} = \frac{\delta D_s}{\delta D_{s-1}} Z^{d_{s-1}} \\ &= \frac{\delta D(D_{s-1})}{\delta D_{s-1}} Z^{d_{s-1}} \end{aligned}$$

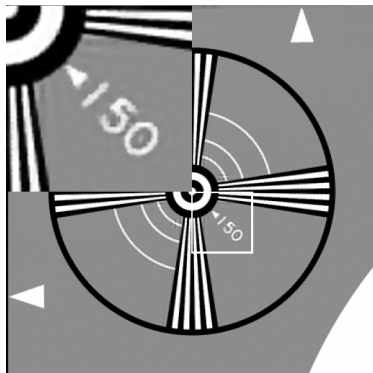
$\frac{\delta D_1(X)}{\delta X}$ is a subgradients of max operator computed easily and then propagate in higher scale.



SR image reconstruction



BTV regularization(PSNR=31.29)



Proposed regularization(PSNR=32.46)

SR image reconstruction



BTV regularization(PSNR=29.80)



Proposed regularization(PSNR=31.45)

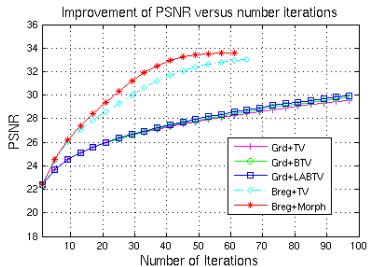


SR image reconstruction : Time Comparison

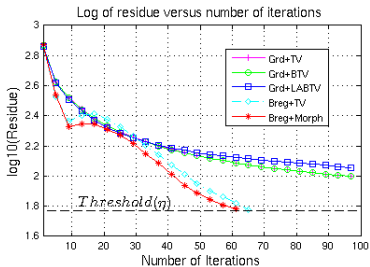
Table: Time comparison of different methods. 10 LR images upsampled with resolution factor 5×5 .

| Method | Grd+TV | Grd+BTV | Grd+LABTV | Breg+TV | Breg+Morph |
|-----------|--------|---------|-----------|---------|------------|
| Iteration | 221 | 211 | 308 | 68 | 63 |
| Time | 19.72s | 32.47s | 290.48s | 6.83s | 12.45s |

Performance comparison

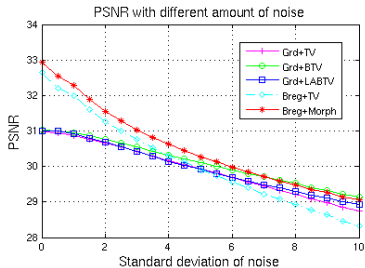


PSNR Vs. # Iteration

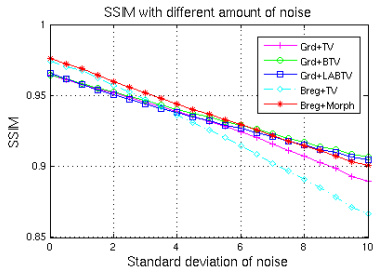


log₁₀(Residue) Vs. # Iteration

Performance comparison

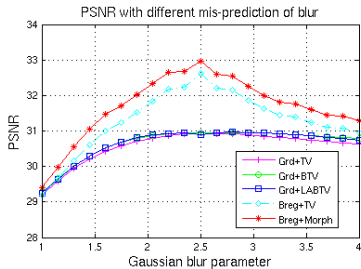


PSNR Vs. noise variation

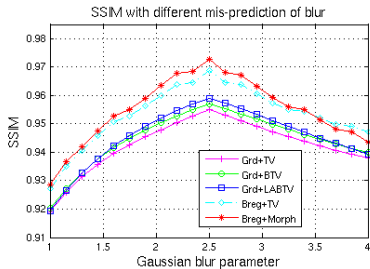


SSIM Vs. noise variation

Performance comparison



PSNR Vs. blurring kernel



SSIM Vs. blurring kernel



Chapter III: Geodesic Kernel smoother for SR image reconstruction.





The non-linear filtering Vs regularization technique

For different kind of regularizer with p^{th} -norm:

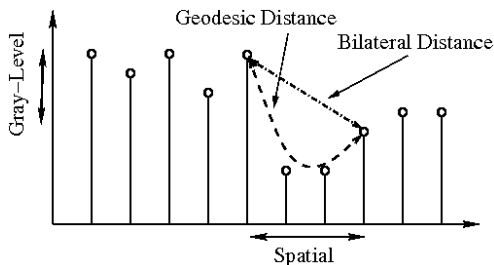
$$\begin{aligned}\Upsilon(X) &= \sum_{l,m \in N_a} \alpha_{lm} \|X - S_x^l S_y^m X\|_p \\ &\geq \|X - \sum_{l,m \in N_a} \alpha_{lm} S_x^l S_y^m X\|_p \\ &\quad \text{(using Jensen's Inequality), for } p > 1 \\ &= \|X - R \otimes X\|_p \\ &\quad \text{(Invariant to non-linear filtering } R, \\ &\quad \text{removes only noise present in the image)}\end{aligned}$$

For 4-N neighbourhood:

$$\begin{aligned}\Upsilon(X) &= \sum_{l,m \in N_g} \alpha_{lm} \|X - S_x^l S_y^m X\|_p \\ &= 2 \|(\nabla_x + \nabla_y)X\|_p \\ &= \|\nabla X\|_p\end{aligned}$$

Existing approximate Kernels:

- ▶ LARK Kernel [Takeda, et al. '07]
- ▶ Beltrami Kernel [Sochen, et al. '98]
- ▶ Structure Tensor [Brox, et al. '04]

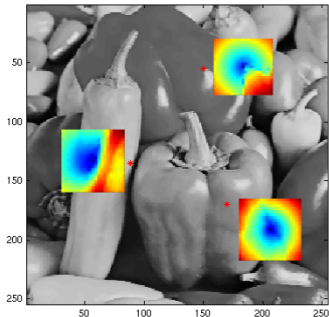


The values of the kernel are computed as:

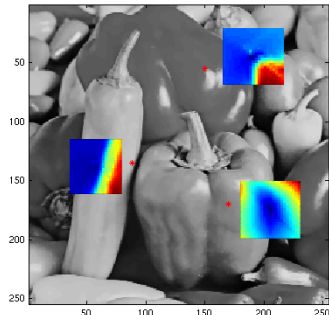
$$K(x, y) = e^{-\frac{\text{distance}(x, y)^2}{\sigma^2}}$$

Figure: Illustrates different kernel representations.

Bilateral Kernel Vs. Geodesic Kernel



Bilateral Kernel



Geodesic Kernel

Visualization of bilateral and geodesic kernels at different points in the image (blue-red represents higher-smaller values of the kernels).



Image smoothing using Bilateral Kernel



Original Image



After one iterations



Image smoothing using Bilateral Kernel



After ten iterations



After twenty iterations



Motivation:

- ▶ Optimal Regularization is always desired.
- ▶ The edge preserving nature of the previous example suggests that Geodesic kernel can preserve better edge structure.
- ▶ Locally adaptive nature best suits for regularization problem.

Difficulty:

- ▶ Non-linear nature results subgradients difficult to compute.
- ▶ Usual Geodesic distance computation is slow.





Challenge for geodesic kernel regularization

Difficulty: Possible Solution

- ▶ Non-linear nature results subgradients difficult to compute.
 - # We use the same idea to compute subgradients as we did for Morphologic Regularization.
- ▶ Usual Geodesic distance computation is slow.
 - # We develop an efficient algorithm to compute Geodesic distance. We also derive split-Bregman iterations for SR image reconstruction using geodesic kernel regularization.



Algorithm:

Our Iterative Algorithm for SR Reconstruction:

Initialize $\mathbf{Z}^{(0)} = \mathbf{V}^{(0)} = \mathbf{U}_k^{(0)} = \mathbf{0}$, $n = 0$, $\mathbf{X}^{(0)} = \sum_{k=1}^K \mathbf{A}_k^T \mathbf{Y}_k$;

While $\sum_{k=1}^K \|A_k \mathbf{X}^{(n)} - \mathbf{Y}_k\| > \epsilon$

$$\begin{cases} \mathbf{X}^{(n+1)} &= \mathbf{X}^{(n)} + \mu \frac{\delta \Upsilon(\mathbf{X})}{\delta \mathbf{X}} \Big|_{\mathbf{X}^{(n)}} (\Upsilon(\mathbf{X}^{(n)}) - \mathbf{Z}^{(n)} - \mathbf{V}^{(n)}) \\ &+ \sum_{k=1}^K A_k^T (A_k \mathbf{X}^{(n)} - \mathbf{Y}_k + \mathbf{U}_k^{(n)}) \\ \mathbf{Z}^{(n+1)} &= \delta * \text{Shrink} (\Upsilon(\mathbf{X}^{(n+1)}) - \mathbf{V}^{(n)}, 1/\mu) \\ \mathbf{V}^{(n+1)} &= \mathbf{V}^{(n)} + (\Upsilon(\mathbf{X}^{(n+1)}) - \mathbf{Z}^{(n+1)}) \\ \mathbf{U}_k^{(n+1)} &= \mathbf{U}_k^{(n)} + (A_k \mathbf{X}^{(n+1)} - \mathbf{Y}_k), \quad \forall k = 1, 2 \dots K \end{cases}$$

$n = n + 1$

end

Result of SR method with geodesic kernel regularization



Figure: Top row : SR image using Bicubic interpolation (PSNR = 25.53dB, SSIM = 0.7936), TV+Grd method[12] (PSNR = 28.58dB, SSIM = 0.8614), BTV+Grd method[1] (PSNR = 28.96dB, SSIM = 0.8653). Bottom row : SR reconstructed image using LABTV+Grd method[5] (PSNR = 29.04dB, SSIM = 0.8712), TV+Breg[6] (PSNR = 31.34dB, SSIM = 0.9135), and proposed method Geo+split-Breg (PSNR = 31.54dB, SSIM = 0.9180)



Result of SR method with geodesic kernel regularization

| Images | Bicubic | TV + Grd[12] | BTV + Grd[1] | LABTV + Grd[5] | TV + Brg[6] | Geo + split-Breg |
|----------|---------|--------------|--------------|----------------|---------------|------------------|
| Man | 25.69 | 29.04 | 29.10 | 28.90 | 31.90 | 32.16 |
| | 0.7328 | 0.8463 | 0.8494 | 0.8529 | 0.9164 | 0.9213 |
| Peppers | 25.55 | 29.67 | 29.66 | 29.86 | 33.71 | 34.28 |
| | 0.8592 | 0.9177 | 0.9185 | 0.9199 | 0.9566 | 0.9599 |
| Barbara | 26.48 | 30.07 | 30.17 | 30.20 | 31.86 | 32.15 |
| | 0.7856 | 0.8627 | 0.8653 | 0.8682 | 0.8999 | 0.9047 |
| Boat | 24.20 | 28.37 | 28.46 | 28.42 | 32.16 | 32.24 |
| | 0.7490 | 0.8589 | 0.8626 | 0.8631 | 0.9386 | 0.9408 |
| Lake | 21.88 | 25.40 | 25.44 | 25.45 | 28.60 | 28.58 |
| | 0.7441 | 0.8596 | 0.8615 | 0.8607 | 0.9267 | 0.9259 |
| Airplane | 23.81 | 28.26 | 28.32 | 28.30 | 32.02 | 32.16 |
| | 0.8106 | 0.8979 | 0.8995 | 0.8999 | 0.9485 | 0.9503 |
| Baboon | 23.37 | 25.13 | 25.24 | 25.35 | 26.72 | 26.85 |
| | 0.5396 | 0.6884 | 0.6963 | 0.7096 | 0.8091 | 0.8162 |
| Couple | 26.29 | 30.12 | 30.21 | 30.24 | 33.71 | 33.91 |
| | 0.7188 | 0.8403 | 0.8450 | 0.8500 | 0.9306 | 0.9346 |
| Splash | 28.37 | 33.86 | 33.90 | 33.74 | 39.57 | 39.50 |
| | 0.9007 | 0.9368 | 0.9374 | 0.9392 | 0.9631 | 0.9667 |
| Tiffany | 26.25 | 32.95 | 32.90 | 32.80 | 36.03 | 36.54 |
| | 0.8640 | 0.9095 | 0.9113 | 0.9124 | 0.9440 | 0.9502 |
| Zelda | 29.57 | 33.53 | 33.56 | 33.58 | 35.88 | 36.32 |
| | 0.8901 | 0.9283 | 0.9299 | 0.9332 | 0.9542 | 0.9597 |
| Bird | 21.82 | 23.58 | 23.62 | 23.65 | 24.99 | 25.02 |
| | 0.7787 | 0.8445 | 0.8466 | 0.8472 | 0.8943 | 0.8998 |

Table: PSNR (dB) AND SSIM OF RECONSTRUCTED SR IMAGES (NOISE LEVEL $\sigma_n = 0$)



Chapter IV: Single-frame Super Resolution with multiple Dictionary learning



Algebraic Image Zooming



Input Image



Nearest Neighbour Interpolated Image

Algebraic Image Zooming



Input Image



Bicubic Interpolated Image

Model-Based Image Zooming



Input Image



Super Resolution Image



State-of-Art:

- ▶ Soft edge smoothness prior [Dai *et al.* 07].
- ▶ Sparse Coding Techniques [Yang *et al.* 08, 10].
- ▶ Self Similarity Measures [Glasner *et al.* 09].



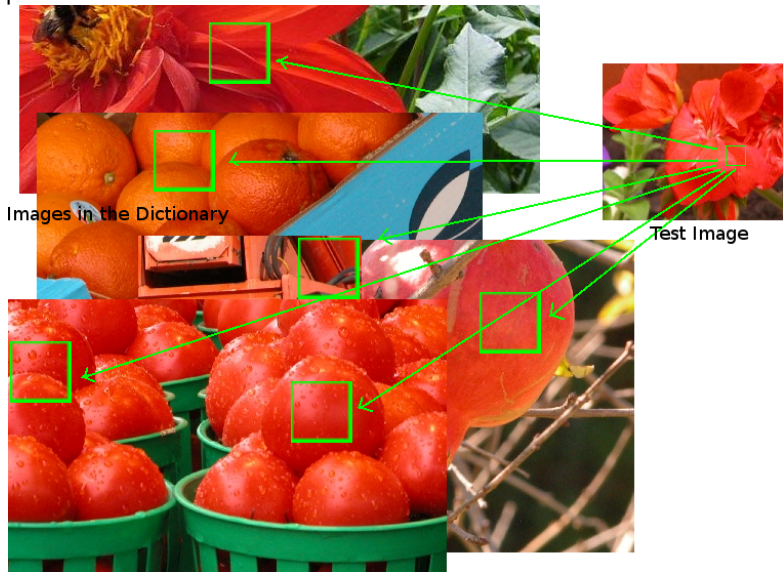


Motivation Behind this work:

- ▶ A blur and down-sampled patch can be generated from multiple possible LR patches.
- ▶ All the existing methods (mostly patch-based techniques) predict sharp patches corresponding to a blur down-sampled patch.
- ▶ Better SR image can be estimated if we predict all the possibilities and choose the best one that suits the neighbourhood patches.



Motivation Behind this work:





Model-Based Image Zooming

Proposed Model:

- ▶ Cluster /Classify patches using Probabilistic Latent Symantic Analysis (pLSA).
- ▶ Use sparse dual dictionary technique to predict HR patch.



Topic Modelling

Topics

gene 0.04
dna 0.02
genetic 0.01
...

life 0.02
evolve 0.01
organism 0.01
...

brain 0.04
neuron 0.02
nerve 0.01
...

data 0.02
number 0.02
computer 0.01
...

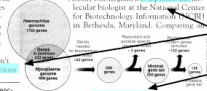
Documents

Seeking Life's Bare (Genetic) Necessities

COLD SPRING HARBOR, NEW YORK—How many genes does an organism need to survive? Last week at the genome meeting here, two genome researchers with radically different approaches presented complementary views of the basic genes needed for life. One research team, using computer analyses to compare known genomes, concluded that today's organisms can be sustained with just 252 genes, and that the earliest life forms required a mere 128 genes. The other researcher mapped genes in a simple parasite and estimated that for this organism, 802 genes are plenty to do the job—but that anything short of 100 wouldn't be enough.

Although the numbers don't match precisely, those predictions

"are not all that far apart," especially in comparison to the 75,000 genes in the human genome, notes Siv Andersson, a genome researcher at the University in Sweden who arrived in the CSH summer, but coming up with a common denominator may be more than just a computer numbers game. Particularly in more and more genomes are currently sequenced and sequenced. "It may be a way of organizing any newly sequenced genomes," explains Aracely Mushegian, a computational molecular biologist at the National Center for Biotechnology Information (NCBI) in Bethesda, Maryland. Computing an

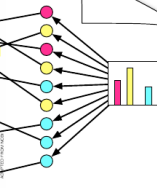


* Genome Mapping and Sequencing, Cold Spring Harbor, New York, May 8 to 12.

Stripping down. Computer analysis yields an estimate of the minimum modern and ancient genomes.

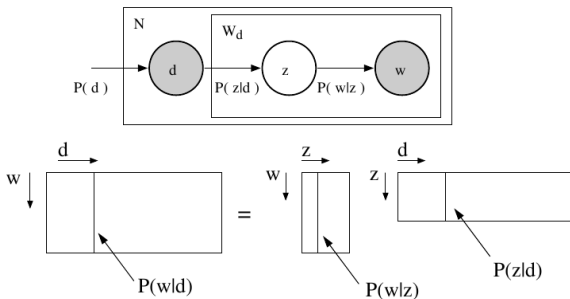
SCIENCE • VOL. 272 • 24 MAY 1996

Topic proportions and assignments



- ▶ Each topic is a distribution of words.
- ▶ Each document is a mixture of topics in corpus.
- ▶ Each word is drawn from one of those topics.

Probabilistic Latent Symantic Analysis (pLSA)



Model Assumption:

$$P(w_i|d_j) = \sum_{k=1}^K P(z_k|d_j)P(w_i|z_k),$$

where $P(z_k|d_j)$ is the probability of topic z_k occurring in document d_j , and $P(w_i|z_k)$ is the probability of word w_i occurring in a particular topic z_k .

Why topic model?

- ▶ It can compute inherent topics (soft-clustering of documents) in unsupervised way.
- ▶ After training it can assign soft-label of topics on test documents.
- ▶ An EM algorithm is used to compute all the probability distributions.

Context of SR:

- ▶ “Document” as cropped portion of an image consisting of smaller patches as called “Words” .
- ▶ “Topic” is a higher level concept (Document consist of smooth regions/ edge regions/ texture regions).

Offline Phase:

- ▶ Collect a set of natural images downloaded from a popular photographic forum.
- ▶ Generate HR and LR document pairs and run a topic learning algorithm. Separate out all the documents based on its topic assignment.
- ▶ For each cluster run a dual sparse dictionary learning algorithm.

Online Phase:

- ▶ For test image, divide it into overlapping documents and infer the topic assignment of each document.
- ▶ Predict HR patch for all LR patches inside the document using the corresponding dual dictionary it assigned to.



Sparse coding approach :

- ▶ Train **coupled dictionary** D_l and D_h of HR and LR **image patches** from similar images.
- ▶ For each patch y in LR image, solve

$$\hat{\alpha} = \arg \min \|\alpha\|_1 \quad \text{subject to} \quad \begin{aligned} \|Fy - FD_l\alpha\|_2^2 &\leq \epsilon_1 \\ \|w - PD_h\alpha\|_2^2 &\leq \epsilon_2 \end{aligned}$$

- ▶ Generate the high-resolution patch $x = D\hat{\alpha}$ Put the patch x into a high-resolution image X_0 .
- ▶ For color images Y channel is upsampled via sparse coding. Other channels are interpolated using bicubic interpolation.

Sparse coding approach :

- ▶ **Patch size** : 5×5 to 10×10 gives good quality image.
- ▶ **Size of dictionary** : depends on size of the patch size (usually greater than dimension of the feature vector). We used 100 and 500 size dictionaries for 5×5 and 10×10 patches respectively.
- ▶ **Dictionary learning** : must be learned on similar type of images. If SR image is generated from sparsely reconstructed patches of a global dictionary then using back-projection solve :

$$X^* = \arg \min_X \|X - X_0\| \text{ subject to } LX = Y$$

X^* is the output SR image.

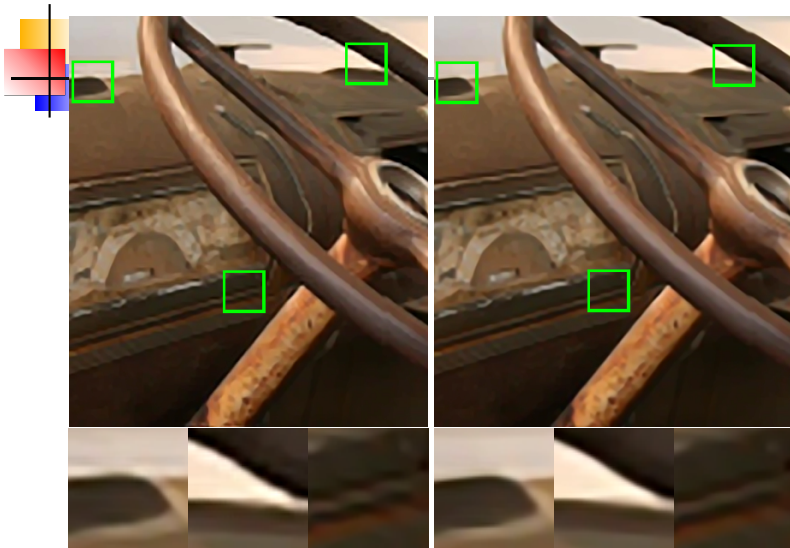
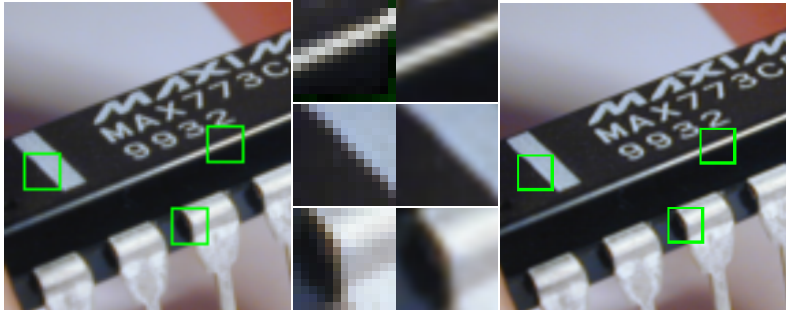
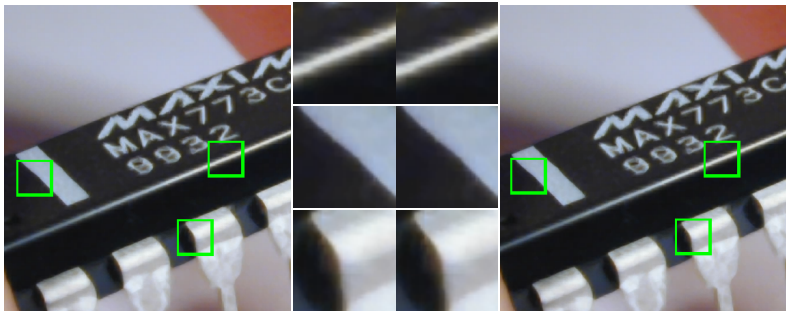


Figure: Using one single global dictionary proposed by Yang *et al.* [14] and proposed method with multiple dictionaries.

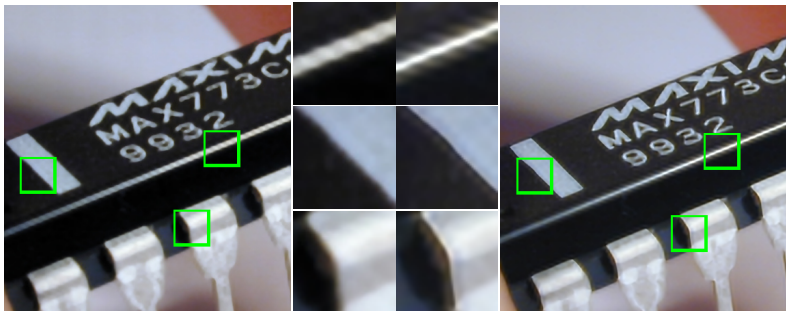


Input image (Scaled for display)

Bicubic interpolation.

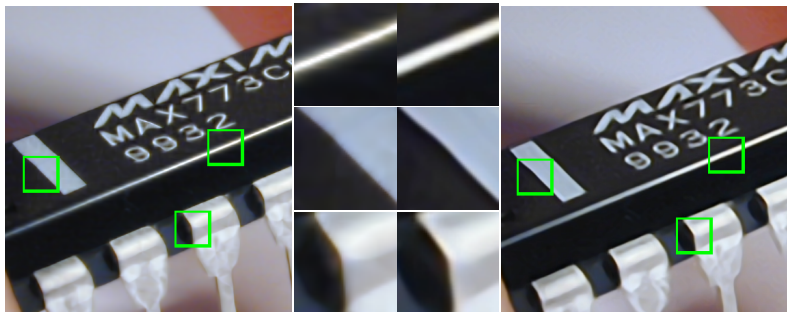


Genuine FractalsTM(commercial product) Sun *et al.* [13]



Fattal *et al.* [2],

Glasner *et al.* [4]



Freeman *et al.* [3]

Proposed method.



Chapter V: Single-frame Super Resolution by exploring local self-similarity between patches.



Motivation:

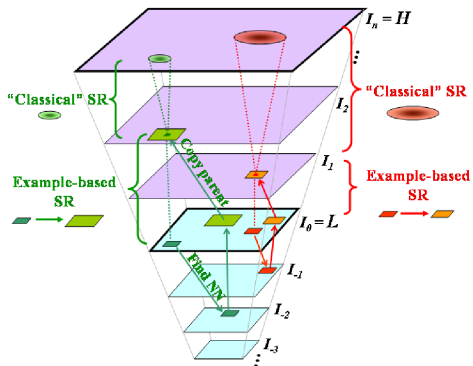
- ▶ Recent study suggest that patches are more tend to re-occur in the image itself in same scale or different scales, rather than patches in the other natural images.
- ▶ This already established in Glasner *et al.* [4] in naive way.

Difficulty:

- ▶ No learning-testing mechanism for LR and HR patch correspondence. Learn online in the image itself.
- ▶ High computation : search nearest neighbour patch for all patches in the down-scaled images.



Glasner et al. technique:



2

²This image taken from Glasner et al. [4]



AN EFFICIENT AND FAST METHOD IS REQUIRED
STILL WORKING ON IT



Document Processing:

- ▶ Off-line Recognition of Hand-Written Bengali Numerals Using Morphological Features, P. Purkait, B. Chanda, *Frontiers in Handwriting Recognition (ICFHR), 2010 International Conference*
- ▶ Writer identification for handwritten telugu documents using directional morphological features, P. Purkait, R. Kumar, B. Chanda, *Frontiers in Handwriting Recognition (ICFHR), 2010 International Conference*

Sketch-Photo synthesis and Recognition:

- ▶ A novel technique for sketch to photo synthesis, P Purkait, S Kulkarni, B Chanda, *Proceedings of the Seventh Indian Conference on Computer Vision, Graphics and Image Processing (ICVGIP), 2010*
- ▶ Face Image Retrieval Based on Probe Sketch Using SIFT Feature Descriptors, K Atal, A Arora, P Purkait, B Chanda, *Perception and Machine Intelligence (PerMin), 2012*



Other Works:

Dance Classification:

- ▶ Indian Classical Dance Classification by Learning Dance Pose Bases, S Samanta, P Purkait, B Chanda, *IEEE Workshop on the Applications of Computer Vision (WACV), 2012*





S. Farsiu, M. D. Robinson, M. Elad, and P. Milanfar.

Fast and robust multiframe super-resolution.

IEEE Trans. Image Process., 13(10):1327–1344, Oct. 2004.



Raanan Fattal.

Image upsampling via imposed edge statistics.

ACM Trans. Graph., 26(3):56–65, Jul. 2007.



Gilad Freedman and Raanan Fattal.

Image and video upscaling from local self-examples.

ACM Trans. Graph., 28(3):1–10, 2010.



Daniel Glasner, Shai Bagon, and Michal Irani.

Super-resolution from a single image.

In *Proceedings of ICCV*, pages 349–356, Oct. 2009.



Xuelong Li, Yanting Hu, Xinbo Gao, Dacheng Tao, and Beijia Ning.

A multi-frame image super-resolution method.

Signal Process., Elsevier, 90(2):405–414, Feb. 2010.





Antonio Marquina and Stanley J. Osher.

Image super-resolution by TV-regularization and Bregman iteration.

J. of Sci. Comput., 37(3):367–382, Dec. 2008.



P. Purkait and B. Chanda.

Morphologic gain-controlled regularization for edge-preserving super-resolution image reconstruction.

Signal, Image and Video Processing, Springer, pages 1–14.



P. Purkait and B. Chanda.

Digital restoration of damaged mural images.

In Proceedings of The 8th Indian Conference on Vision, Graphics and Image Processing (ICVGIP-12) Submitted, December 2012.



P. Purkait and B. Chanda.

Image upscaling using multiple dictionaries of natural image patches.



 P. Purkait and B. Chanda.

Regularization using geodesic kernel smoother for super resolution image reconstruction.

Unpublished (On preparation), PP:1, 2012.

 P. Purkait and B. Chanda.

Super resolution image reconstruction through bregman iteration using morphologic regularization.

IEEE Trans. Image Process., 21(9):–, 2012.

 L. Rudin, S. Osher, and E. Fatemi.

Nonlinear total variation based noise removal algorithms.

Physica D, 60(1-4):259–268, Nov. 1992.

 Jian Sun, Zongben Xu, and Heung-Yeung Shum.

Image super-resolution using gradient profile prior.

In *Proceedings of CVPR*, pages 1–8, Jun. 2008.



Jianchao Yang, John Wright, Thomas S. Huang, and Yi Ma.
Image super-resolution via sparse representation.

IEEE Trans. Image Process., 19(11):2861–2873, Nov. 2010.





Thanks !

